Comprehensive Simulations of Bursting and Non-Bursting Alfvén Waves in ICRF-Heated Tokamak Plasmas

J. Wang[1], Y. Todo[1], R. Seki[1], A. Bierwage[2], N. Tsujii[3], Z. Cheng[1,4],

K. Ogawa[1,5], H. Wang[1], M. Sato[1] and Z.X. Wang[6]

[1]*National Institute for Fusion Science, Toki, Japan*
[2]*National Institutes for Quantum Science and Technology, Rokkasho Institute for Fusion Energy, Aomori, Japan*
[3]*The University of Tokyo, Kashiwa, Japan*
[4]*Zhejiang University, Hangzhou, China*
[5]*The Graduate University for Advanced Studies, SOKENDAI, Toki, Japan*
[6]*Dalian University of Technology, Dalian, China*

30th IAEA Fusion Energy Conference (FEC 2025)

13-18 Oct. 2025, Chengdu, China

Outline

- **Introduction**

- **Simulation model and techniques to achieve a long time scale**

- **Simulation results**

  – **Multi-n simulation of bursting shear Alfvén waves**

  – **Single-n simulation of bursting shear Alfvén waves**

  – **Non-bursting shear Alfvén waves during outboard heating**

- **Summary**
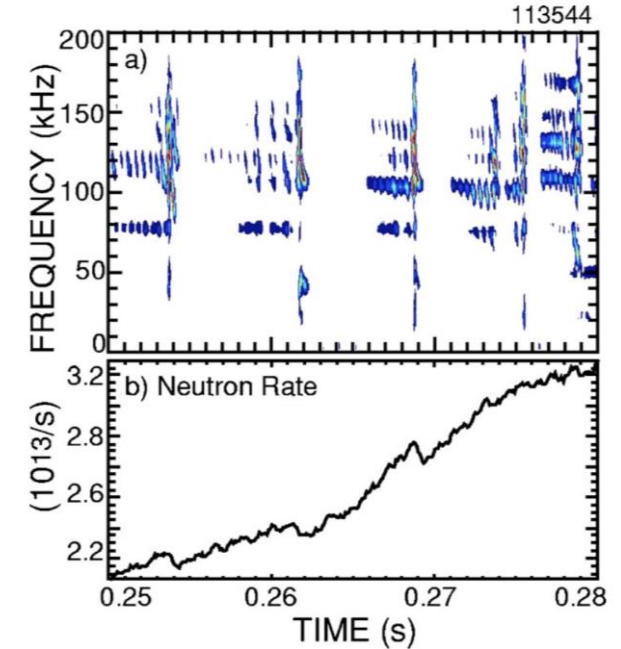
Bursting Alfvén Waves in TFTR
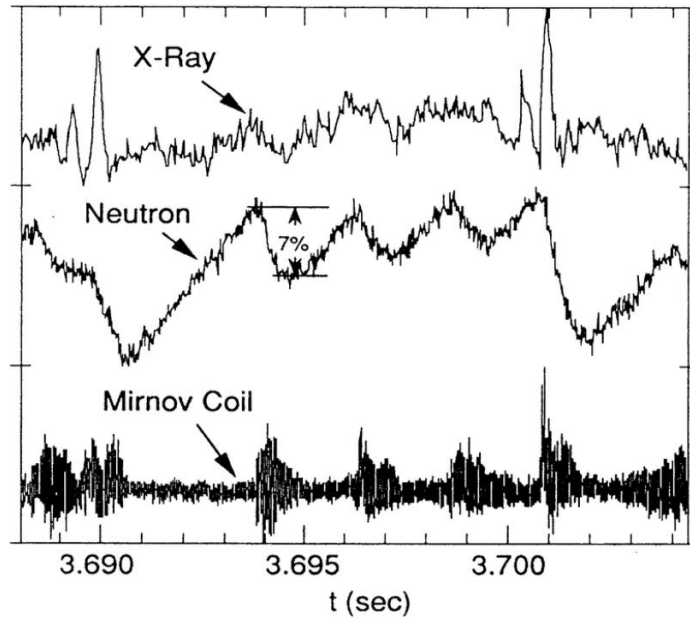
Abrupt Large Events (ALEs) in JT-60U

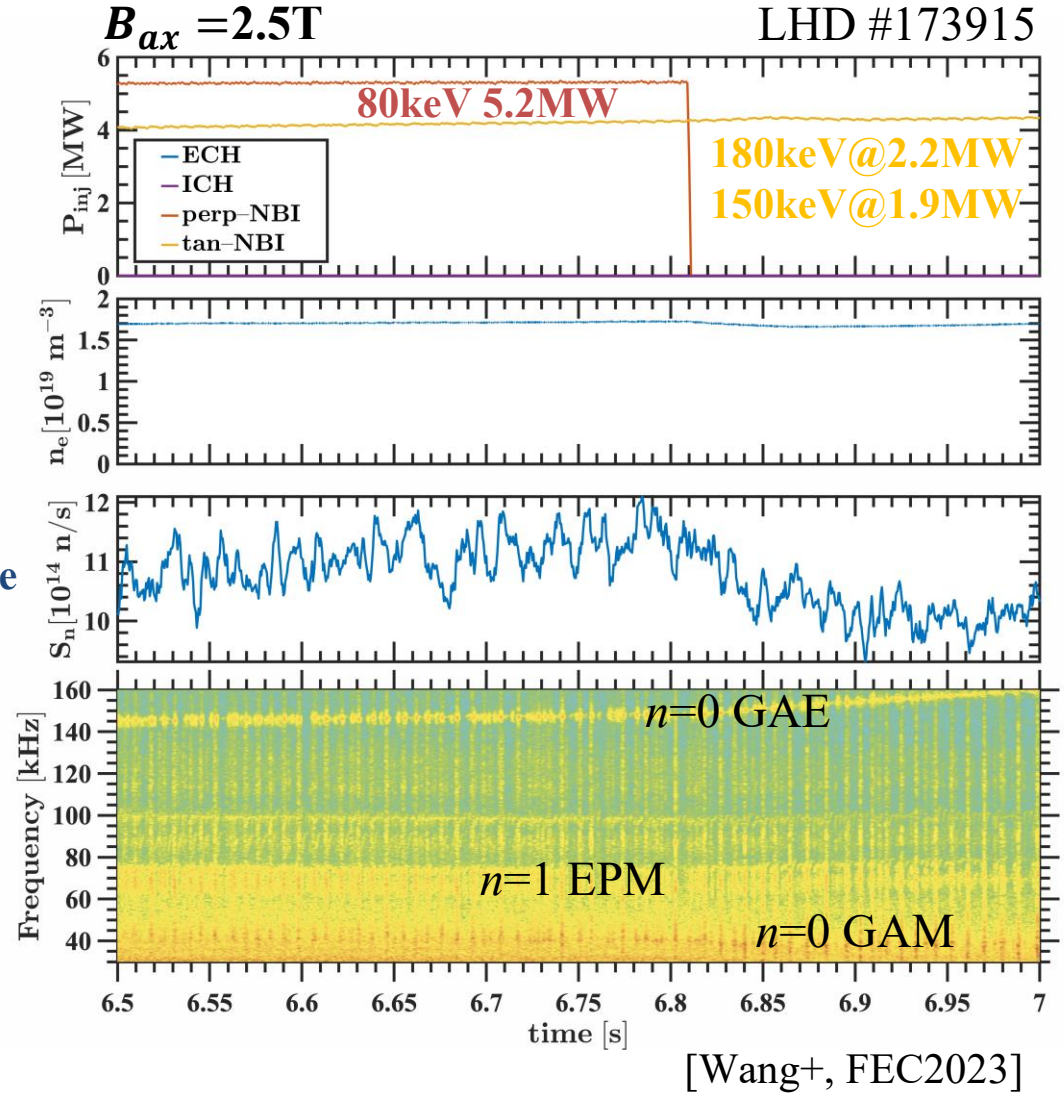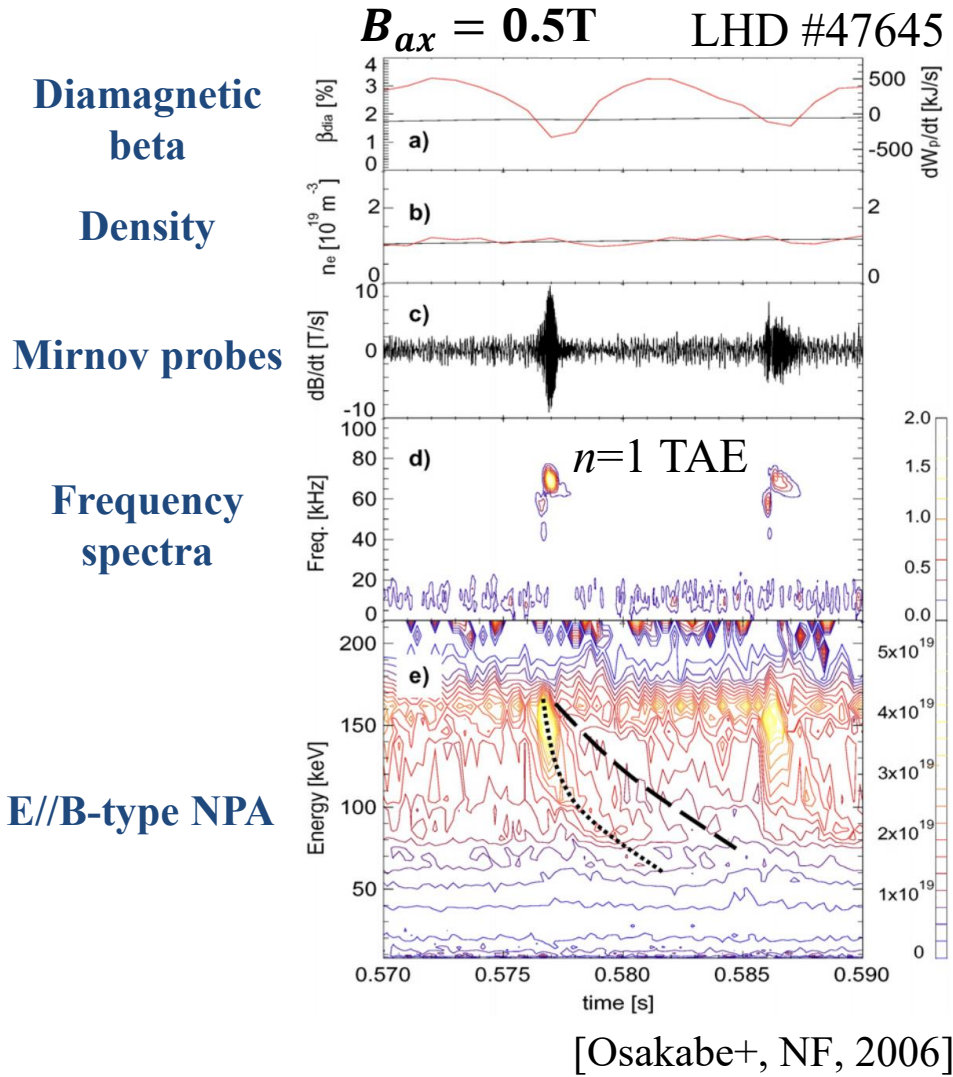**EPM Avalanche in NSTX**

[Wong+, PRL, 1991]
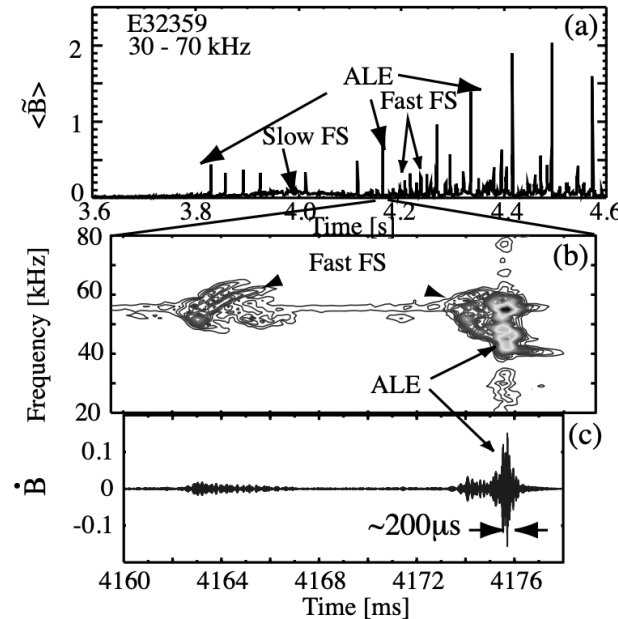
[Shinohara+, NF, 2001]

[Fredrickson+, PoP, 2005]

- **Incompressible shear Alfvén waves (SAWs) are deleterious to the performance of burning plasmas.**

- **SAWs in NBI heated plasma often exhibit a bursting state in present-day tokamaks.**

- **Recurrent bursting Alfvénic instabilities will lead to a rapid and violent release of stored free energy.**

B_{ax} = 0.5T   LHD #47645

Diamagnetic beta

Density

Mirnov probes

Frequency spectra

E//B-type NPA

n=1 TAE

[Osakabe+, NF, 2006]

B_{ax} =2.5T   LHD #173915

Auxiliary heating

80keV 5.2MW

180keV@2.2MW
150keV@1.9MW

ECH
ICH
perp-NBI
tan-NBI

Density

Neutron rate

Frequency spectra

n=0 GAE

n=1 EPM

n=0 GAM

[Wang+, FEC2023]

- **NBI-induced bursts are also routinely observed in LHD for both low and high filed discharges .**

Resonance overlap

Critical EP gradient in phase space

MEGA reproduced SAW bursts in TFTR & DIII-D

[Todo+, NF12, NF14, NF16, NF19, NJP16]
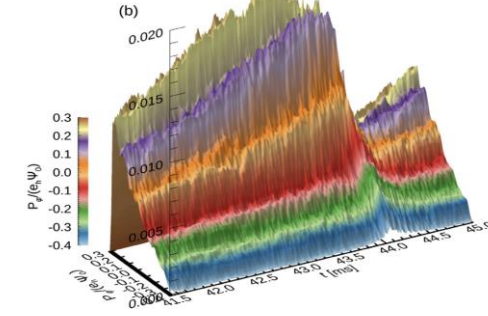
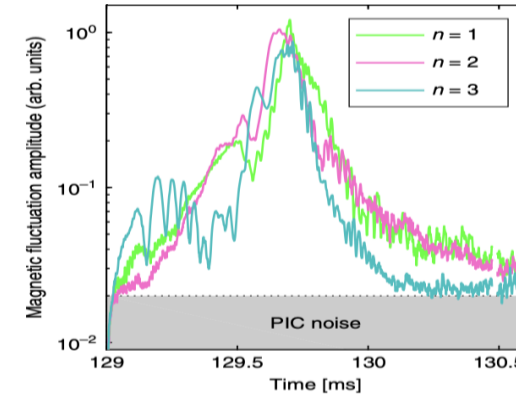**MEGA reproduced ALE in JT-60U**

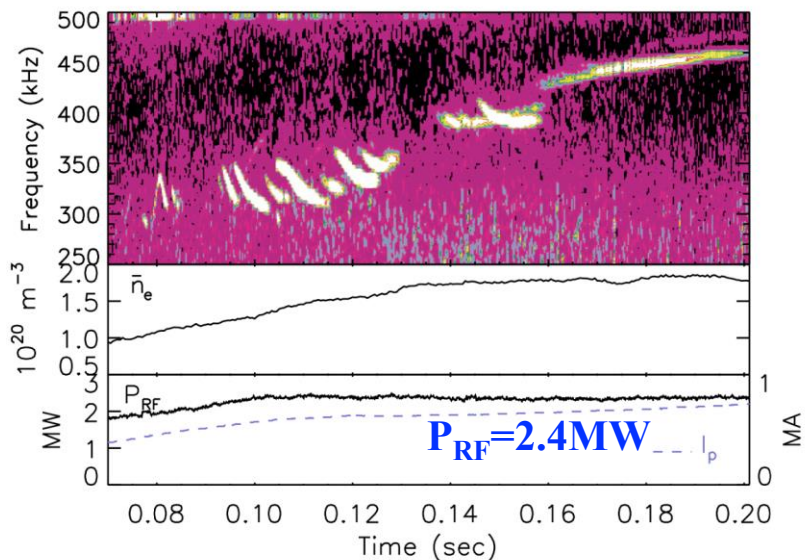[Bierwage+, Nat. Comm., 2018]
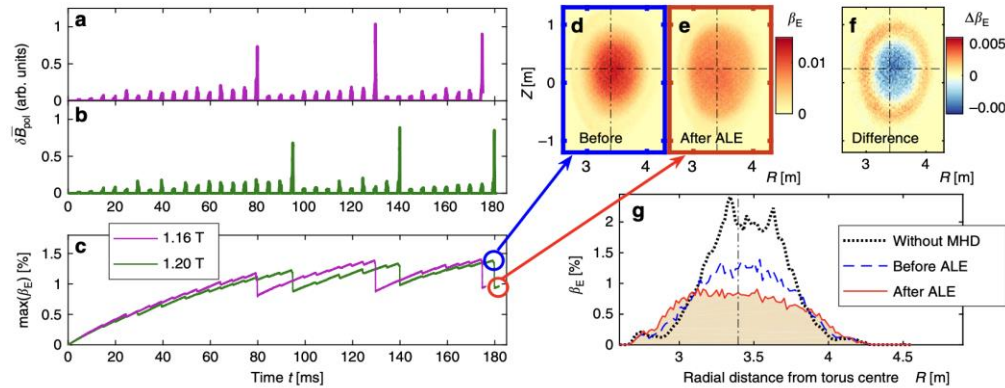
Multiple mode coupling

- **Comprehensive simulations of NBI-induced bursts were simulated by MEGA in a collisional slowing down time scale.**

- **It is revealed that resonance overlap, critical EP gradient in phase space, and multiple mode coupling are key factors.**
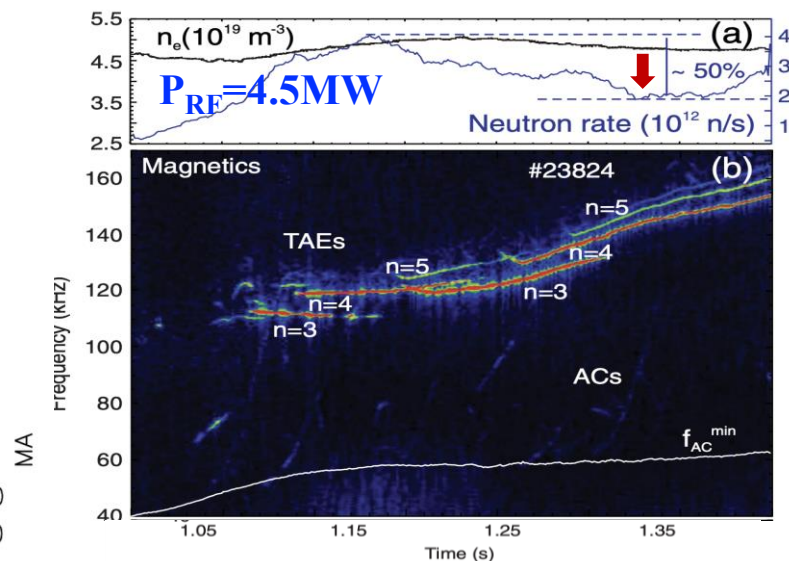
ICRF-induced AEs in C-Mod

[Snipes+, PPCF, 2000]

ICRF-induced TAEs in AUG

P_{RF}=4.5MW

[Garcia-Munoz+, PRL, 2010]

AE States in JET ICH Plasmas

[Heeter+,PRL, 2000]

Theoretical predicted Nonlinear States
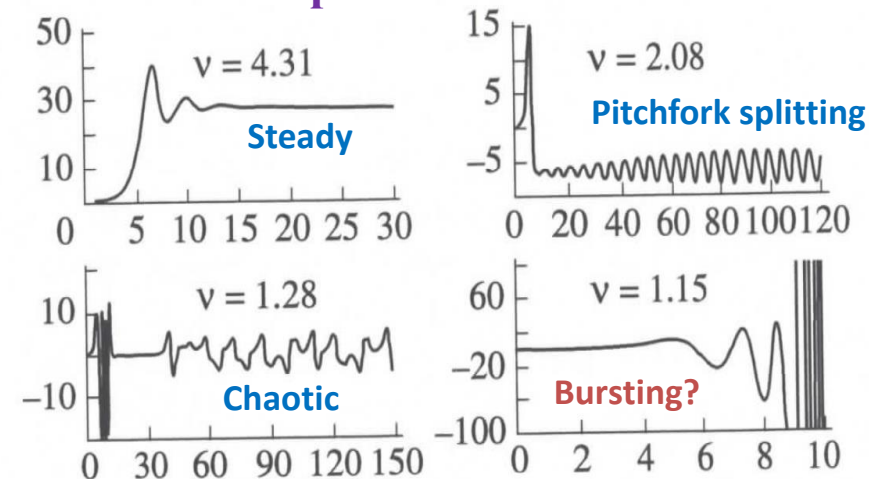
[Berk+, Plasma Physics Reports, 1997]

- Unlike beam-driven SAWs often with bursting behavior, ICRF-induced SAWs, with strong velocity space diffusion, generally have steady amplitude, pitchfork splitting state, or chaotic state.

- ICRF-induced SAWs can be well explained by famous Berk-Breizman-Pekker model based on near-marginal 1-D bump-on-tail instability, except predicted bursting state.

- Mechanism that preventing ICRF-induced SAWs being bursting could open a new avenue for bursting-AE control in burning plasmas.

Bulk plasma (Fluid)

$$\frac{\partial \rho}{\partial t} = -\nabla \cdot (\rho \mathbf{v}) + \nu_n \triangle(\rho - \rho_{eq}),$$

$$\rho \frac{\partial}{\partial t} \mathbf{v} = -\rho \boldsymbol{\omega} \times \mathbf{v} - \rho \nabla(\frac{v^2}{2}) - \nabla p + (\mathbf{j} - \mathbf{j}_h') \times \mathbf{B}$$

$$- \nabla \times (\nu \rho \boldsymbol{\omega}) + \frac{4}{3} \nabla (\nu \rho \nabla \cdot \mathbf{v}),$$

$$\frac{\partial \mathbf{B}}{\partial t} = -\nabla \times \mathbf{E},$$

$$\frac{\partial p}{\partial t} = -\nabla \cdot (p\mathbf{v}) - (\gamma - 1)p\nabla \cdot \mathbf{v} + (\gamma - 1)$$

$$\times [\nu \rho \omega^2 + \frac{4}{3} \nu \rho (\nabla \cdot \mathbf{v})^2 + \eta \mathbf{j} \cdot (\mathbf{j} - \mathbf{j}_{eq})] + \nu_n \triangle(p - p_{eq}),$$

$$\mathbf{E} = -\mathbf{v} \times \mathbf{B} + \eta(\mathbf{j} - \mathbf{j}_{eq}),$$

$$\boldsymbol{\omega} = \boldsymbol{\nabla} \times \mathbf{v},$$

$$\mathbf{j} = \frac{1}{\mu_0} \nabla \times \mathbf{B},$$

E, B →

← **j_h**

Energetic particle (drift kinetic)

$$\mathbf{u} = \mathbf{v}_\parallel^* + \mathbf{v}_E + \mathbf{v}_B,$$

$$\mathbf{v}_\parallel^* = \frac{v_\parallel}{B^*}(\mathbf{B} + \rho_\parallel B \nabla \times \mathbf{b}),$$

$$\mathbf{v}_E = \frac{1}{B^*}(\mathbf{E} \times \mathbf{B}),$$

$$\mathbf{v}_B = \frac{1}{Z_h e B^*}(-\mu \nabla B \times \mathbf{b}),$$

$$\rho_\parallel = \frac{m_h v_\parallel}{Z_h e B},$$

$$\mathbf{b} = \mathbf{B}/B,$$

$$B^* = B(1 + \rho_\parallel \mathbf{b} \cdot \nabla \times \mathbf{b}),$$

$$m_h v_\parallel \frac{dv_\parallel}{dt} = \mathbf{v}_\parallel^* \cdot (Z_h e \mathbf{E} - \mu \nabla B),$$

$$\mathbf{j}_h' = \int (\mathbf{v}_\parallel^* + \mathbf{v}_B) Z_h e f d^3v - \nabla \times \int \mu \mathbf{b} f d^3v,$$
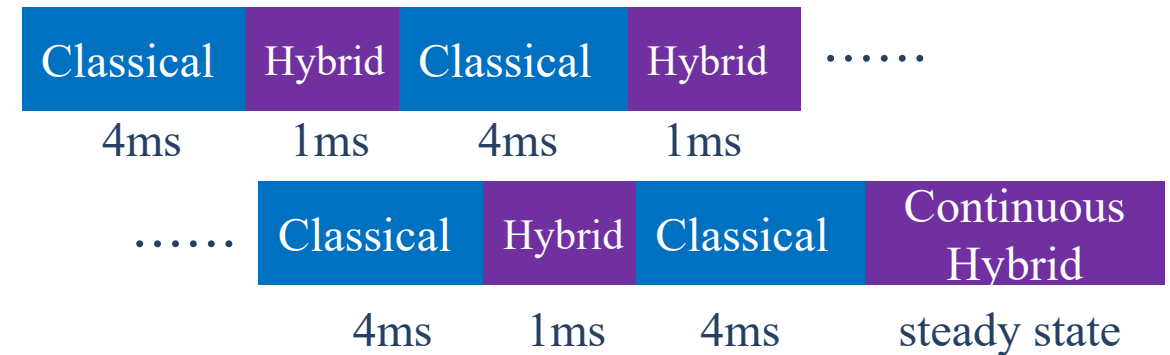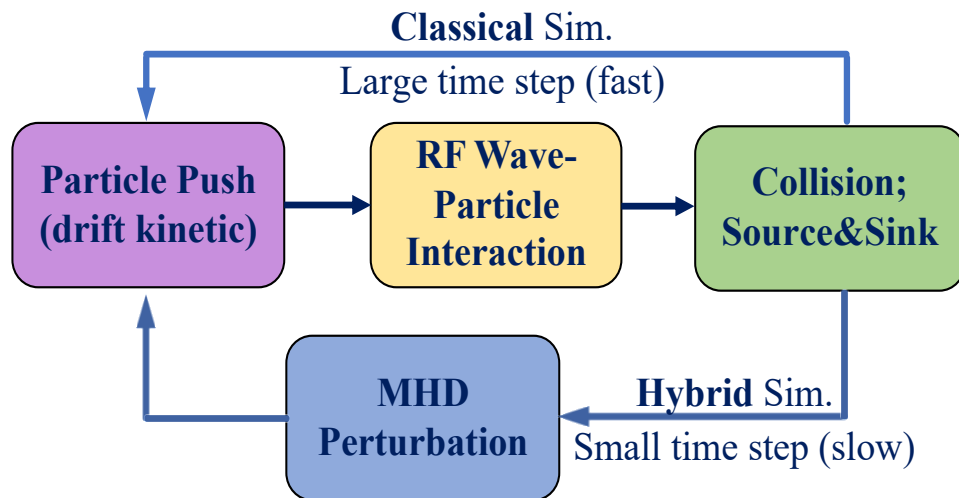
[Y. Todo & T. Sato, PoP, 1998]

- Energetic particle (drift kinetic) contribution is included in MHD momentum equation.

- Equations are solved using fourth-order Runge-Kutta and finite difference schemes in cylindrical coordinates (R, φ, Z).

- FLR effect is neglected to save simulation resource, regardless of MeV particles.

- **SAW nonlinear states** are determined by an interplay between **SAW electric field that flattens** fast ion distribution function and **relaxation processes that restore** the distribution function.
- MEGA code is extended with **ICRF kick, Coulomb collisions, minority ion source and sink**.
- RF kick is based on a quasi-linear theory [Stix, NF, 1975; Murakami+, NF, 2006].
- Both **RF kick** and **Coulomb collisions** are simulated by the **Monte Carlo method**.
- Minority ions are simulated using a **full-f** particle-in-cell method [~0.5 billion markers].
- Sim. setup: $B_0 = 1.5\text{T}$, $R_0/a = 2.6\text{m}/0.9\text{m}$, $n_0 = 3.0 \times 10^{19}\text{m}^{-3}$, $T_0 = 8\text{keV}$, $n^{(H)}/n^{(D)} = 4\%$.
- A parabolic safety factor profile $q(r/a) = q_0 + (q_a - q_0) \cdot (r/a)^2$ with $q_0 = 1.2$ and $q_a = 3.0$.
- A modelled ICRF wave electric field profile is adopted for simplicity with $k_\parallel = 6 \text{ m}^{-1}$.
- **Multi-phase simulation**: **alternately** run classical and hybrid simulations until a steady state.
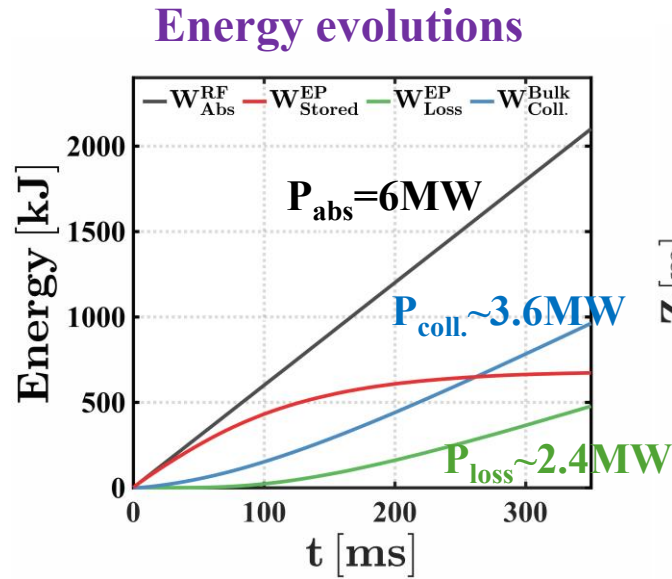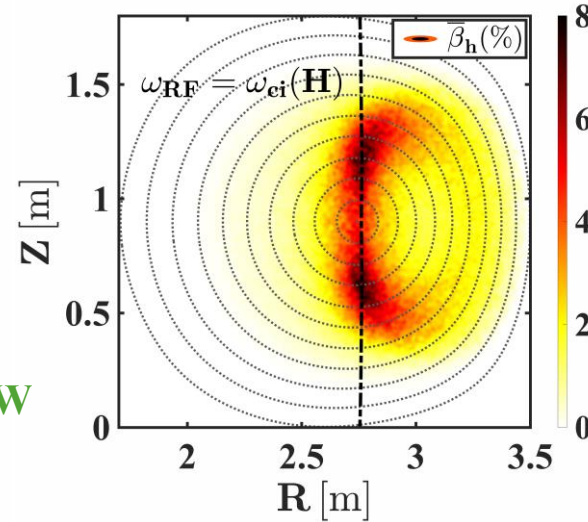

Classical Sim.
Large time step (fast)

Particle Push (drift kinetic) → RF Wave-Particle Interaction → Collision; Source&Sink

MHD Perturbation

Hybrid Sim.
Small time step (slow)

Classical	Hybrid	Classical	Hybrid	......
4ms	1ms	4ms	1ms	

......	Classical	Hybrid	Classical	Continuous Hybrid
	4ms	1ms	4ms	steady state

*Reduce computational time to 1/5 !

Energy evolutions

Minority hydrogen beta

Velocity space distribution
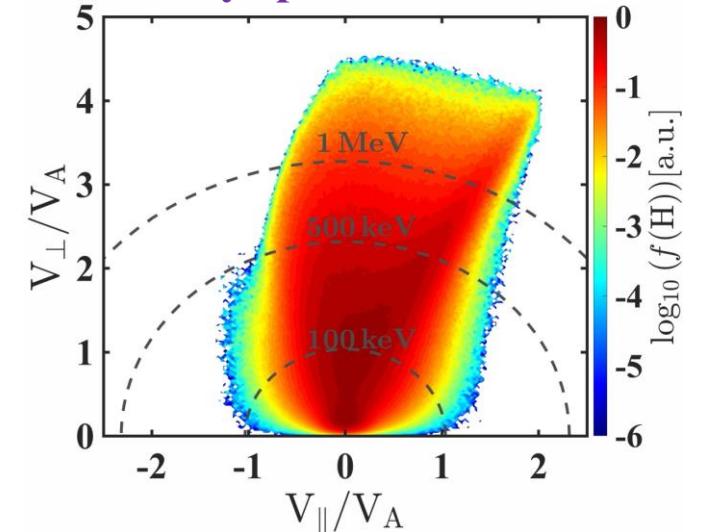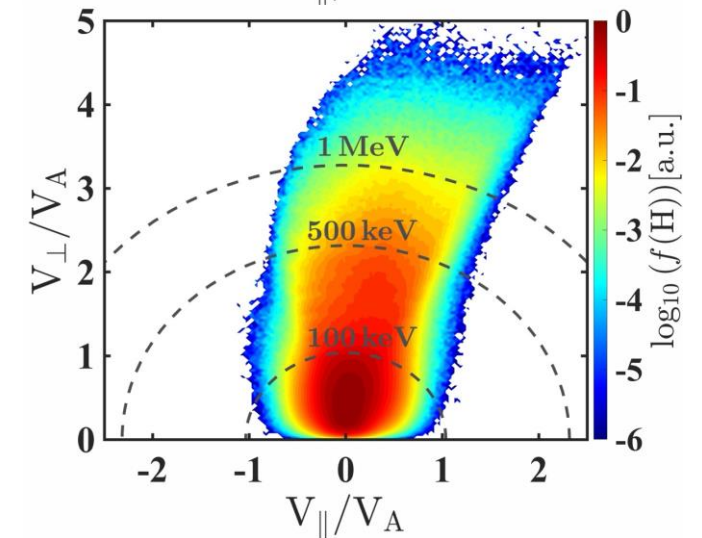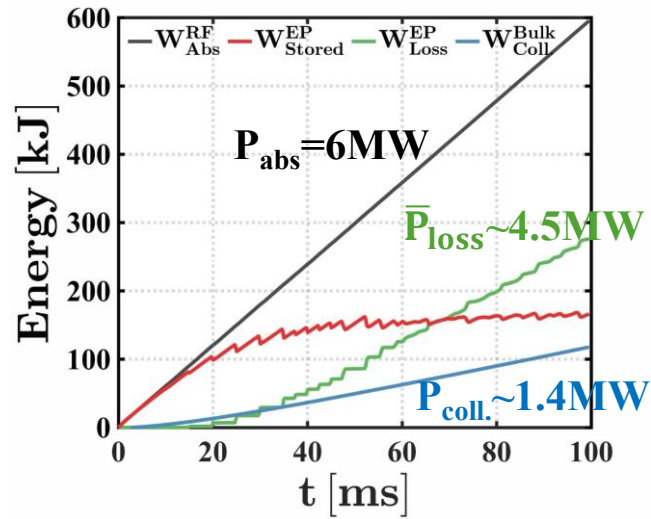
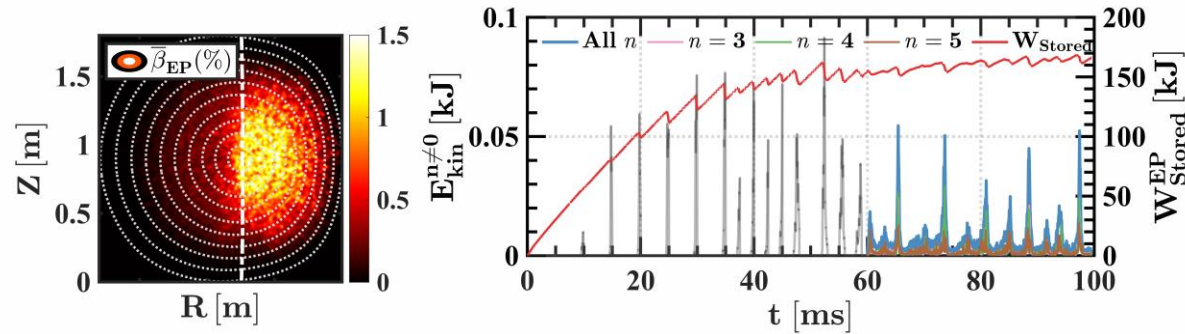Classical simulation

Multi-phase simulation
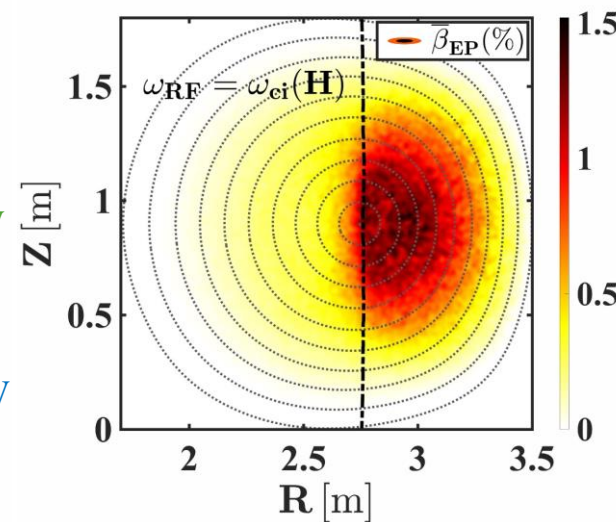
- **Steady-state minority ion distribution in classical simulation is seriously overestimated.**

Outline

- **Introduction**

- **Simulation model and techniques to achieve a long time scale**

- **Simulation results**

  - **Multi-n simulation of bursting shear Alfvén waves**

  - **Single-n simulation of bursting shear Alfvén waves**

  - **Non-bursting shear Alfvén waves during outboard heating**
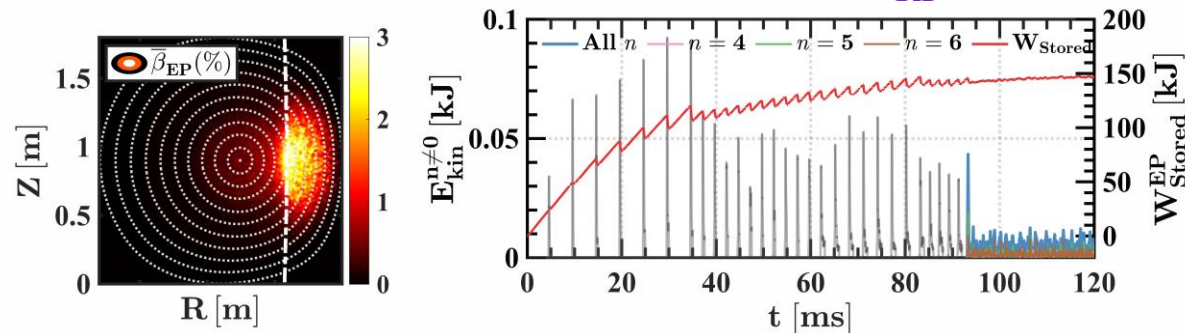
- **Summary**

On-axis ICRF heating with P_{RF}=6MW


Minority energy distribution

Outboard ICRF heating with P_{RF}=6MW
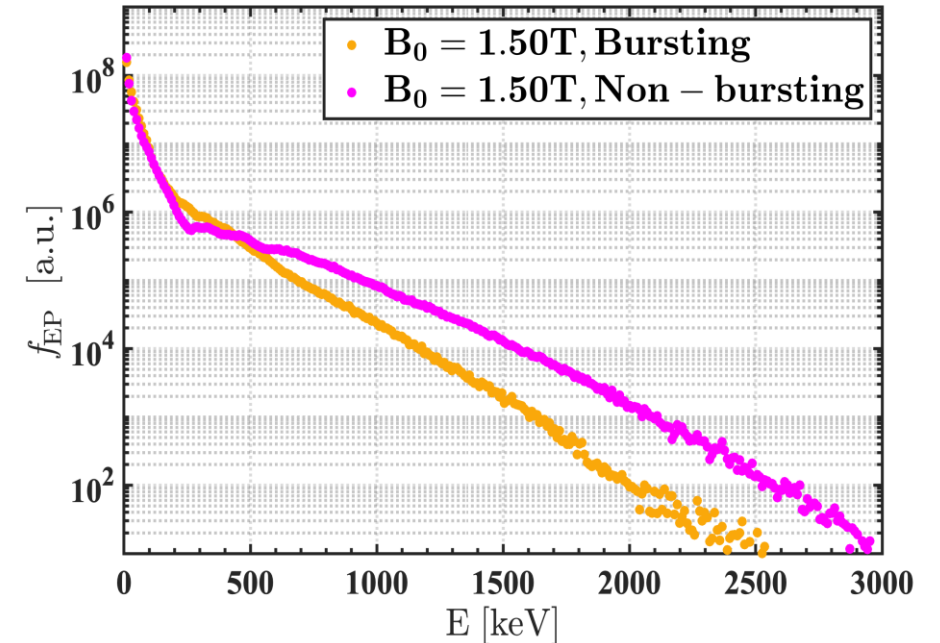
- **Bursting SAWs** are observed when RF resonance layer is located **at the magnetic axis [or inboard]**.
- When RF resonance layer is located at the **outboard** region, only **non-bursting/grassy modes** are observed.
- Non-bursting case has a much higher EP beta and stronger tail ions.
- Noted that nonlinear states can only be identified during the continuous hybrid simulation phase.

MHD kinetic energy evolutions

$\delta\overline{\beta}_{EP}$
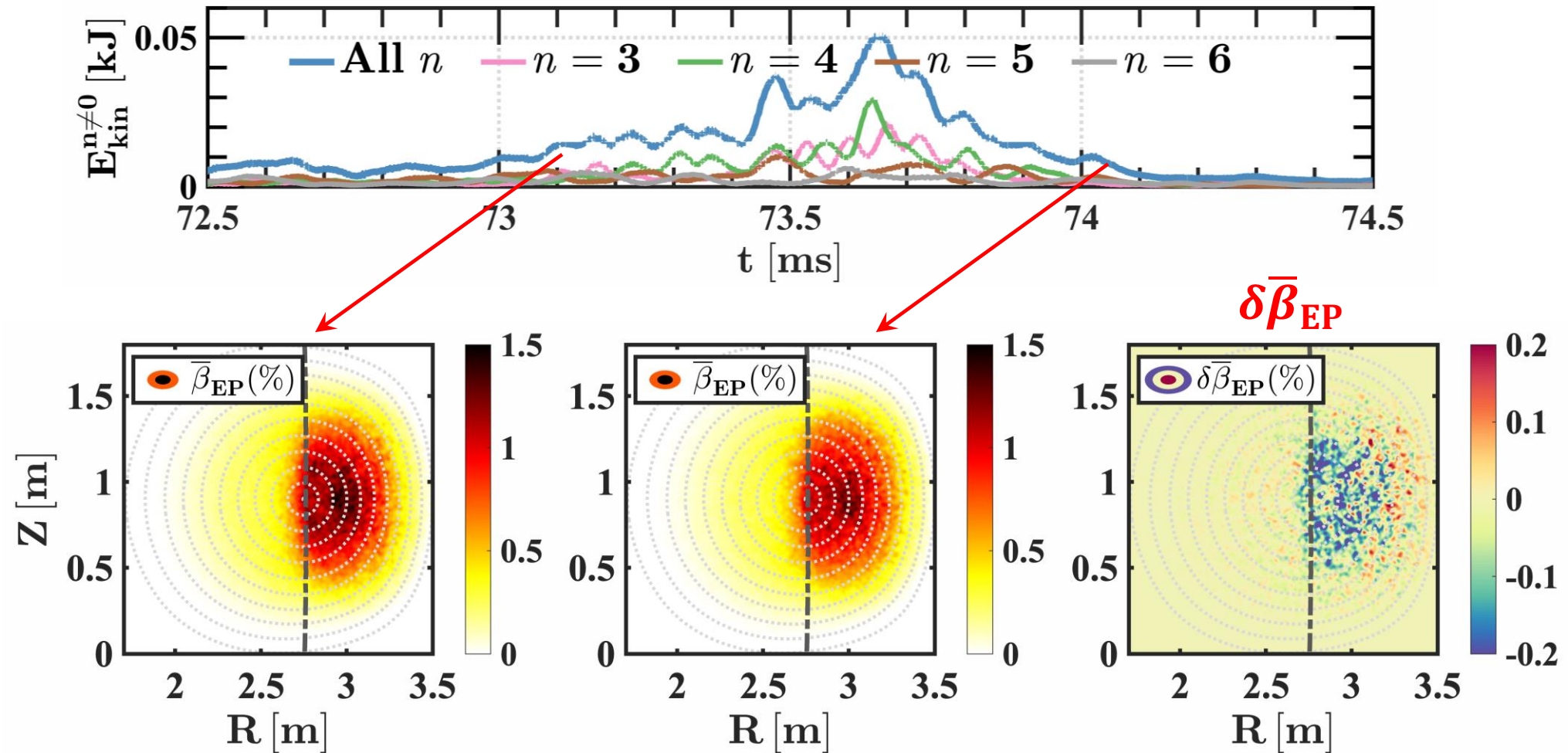
- **About 10% of EPs are transported from the inner to the outer region during the burst.**

MHD kinetic energy evolutions during one burst
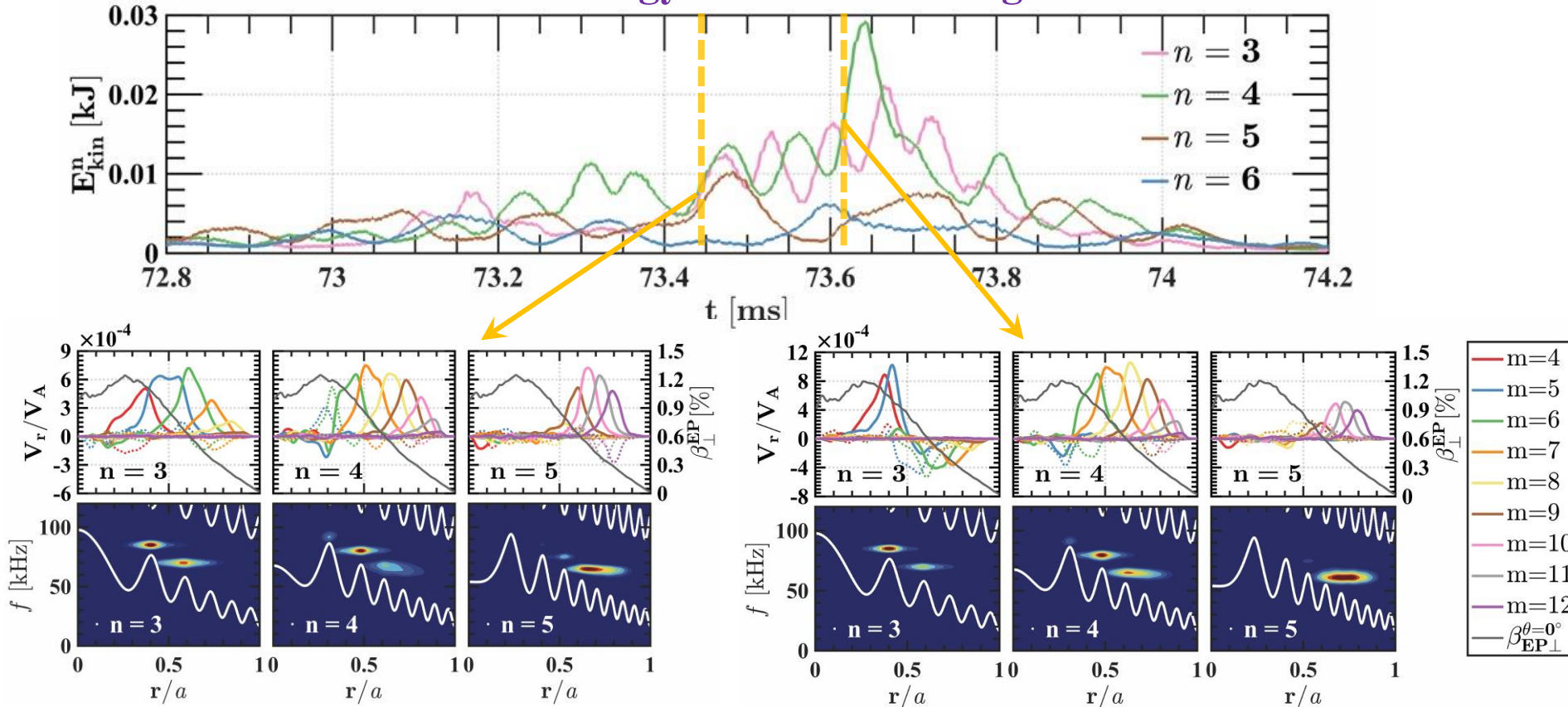
NBI-induced burst (EPMs)

[A. Bierwage+, *Nat. Comm.*, 2018]
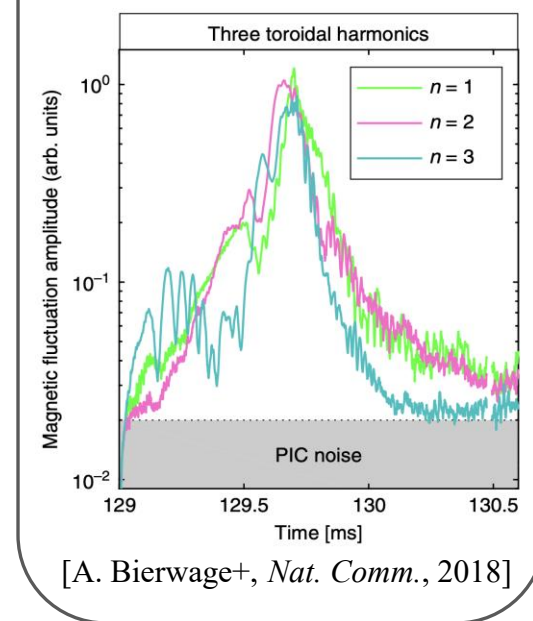
- **Onset and end time of primary modes are similar, which confirms an interaction between different toroidal harmonics. The decay phase of oscillatory growth for each *n* is pronounced.**

- **Discrete TAEs above Alfvén continuum tips are formed for each toroidal harmonic.**

- **There is a spatial overlap region between adjacent TAEs.**

RF wave kick in $v_\perp$ ➡ Deeply trapped EPs: wave-particle res. condition: $\omega_0 \approx n \cdot \omega_d$ ($\omega_d \propto E/q_{loc}$)

Same n (n=3)

$85 \text{ kHz} * \frac{4.5/3}{5.5/3} = 70 \text{ kHz}$

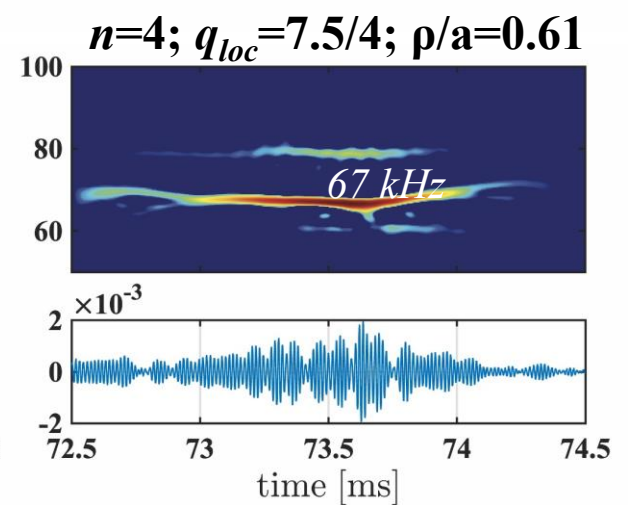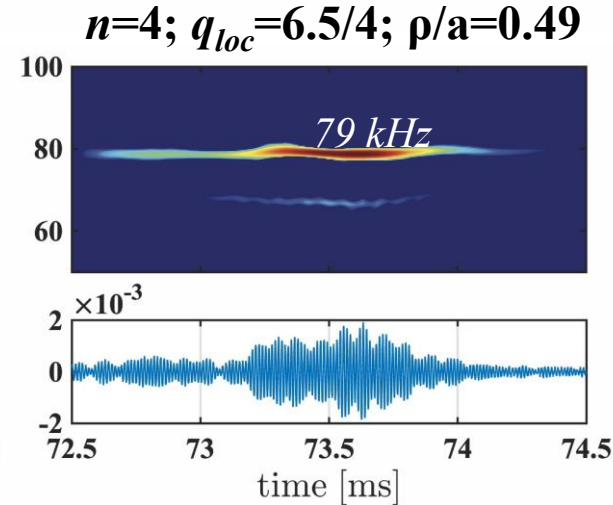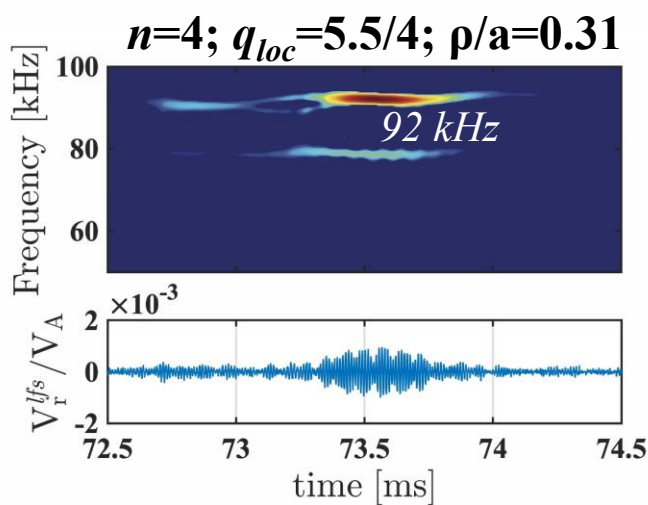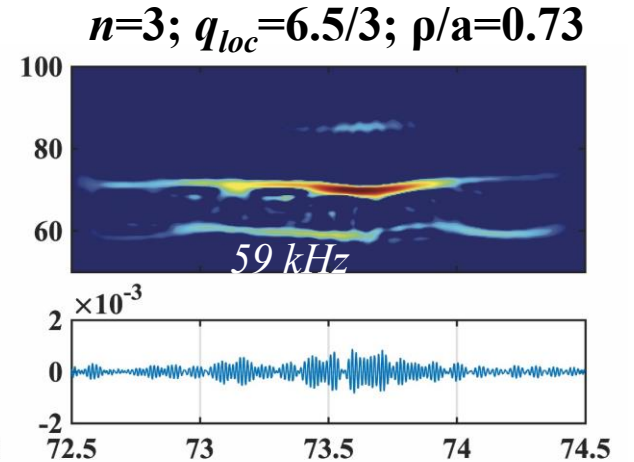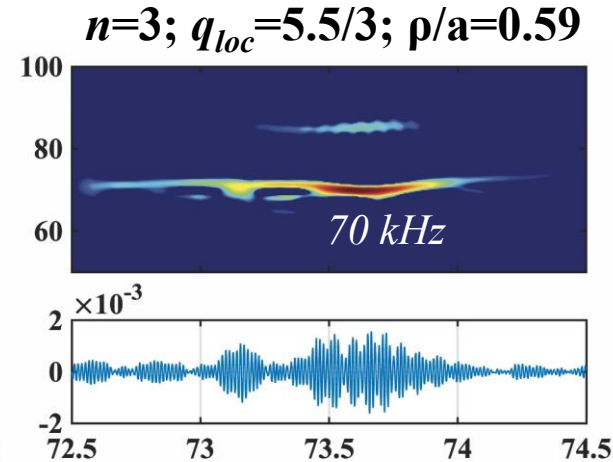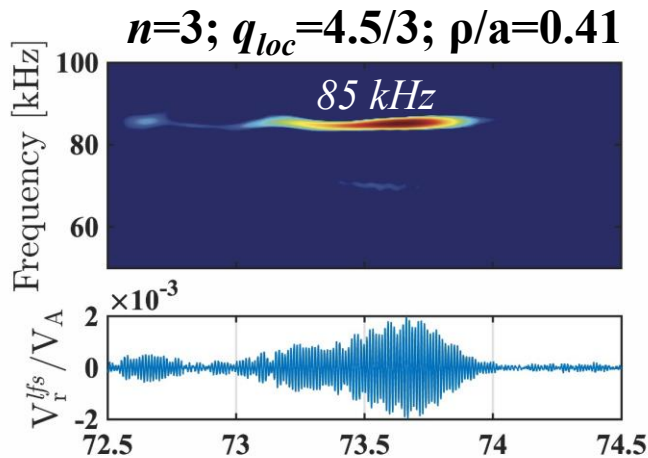$70 \text{ kHz} * \frac{5.5/3}{6.5/3} = 59 \text{ kHz}$

Same n (n=4)

$92 \text{ kHz} * \frac{5.5/4}{6.5/4} = 78 \text{ kHz}$

$79 \text{ kHz} * \frac{6.5/4}{7.5/4} = 68 \text{ kHz}$

Cross n

$92 \text{ kHz} * \frac{5.5/4}{5.5/3} = 69 \text{ kHz}$

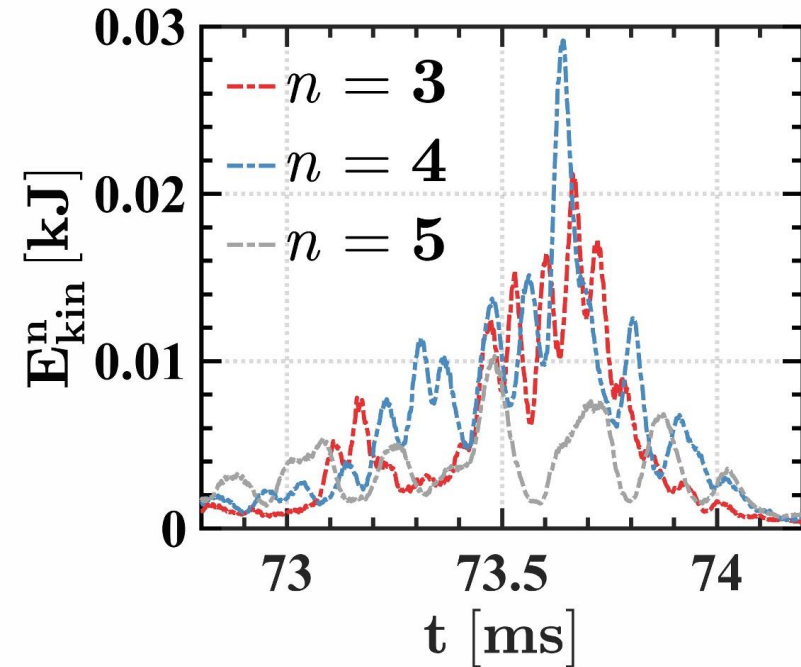$79 \text{ kHz} * \frac{6.5/4}{6.5/3} = 59 \text{ kHz}$

- **Discrete and non-chirping TAEs of each toroidal harmonic are destabilized by a similar group of minority ions in terms of energy and magnetic moment.**
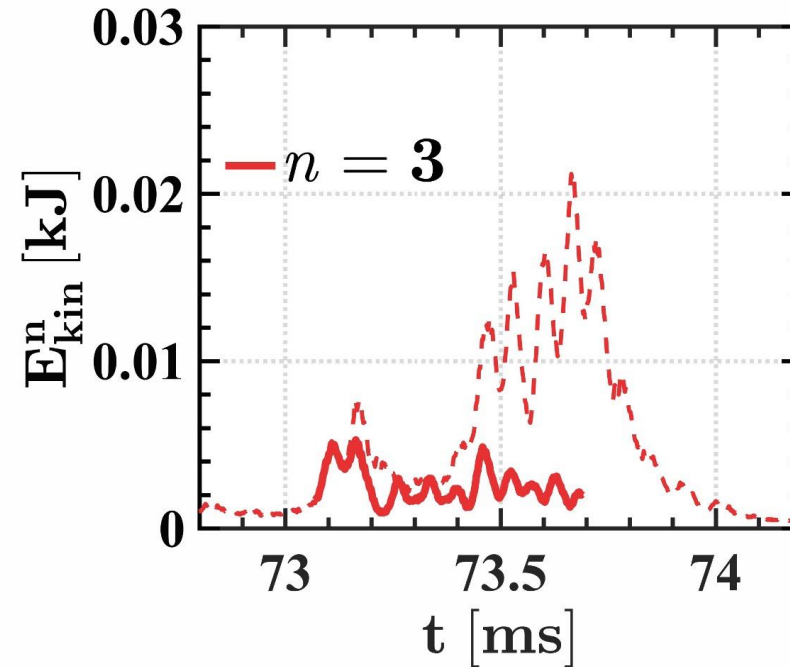
Original multi–*n* simulation

Repeated simulation from 73.07ms with only *n*=3

Repeated simulation from 73.07ms with only *n*=4
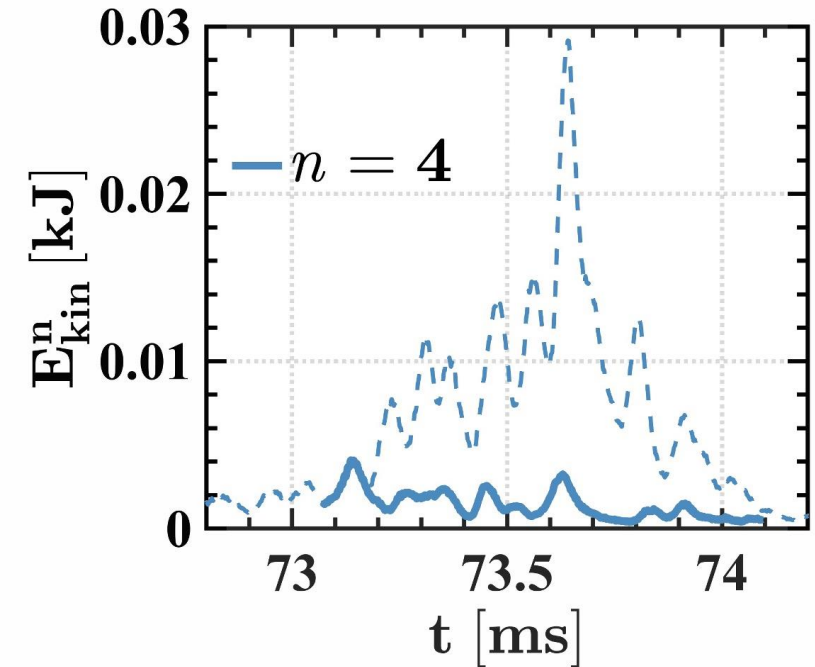
- We repeated simulation at the onset of burst with including only one toroidal harmonic at a time.

- Although the burst is primarily dominated by only two toroidal harmonics (*n*=3 and *n*=4), the inclusion of a single *n* alone is insufficient to induce a burst.

- However, is synergy of different toroidal harmonics really indispensable?

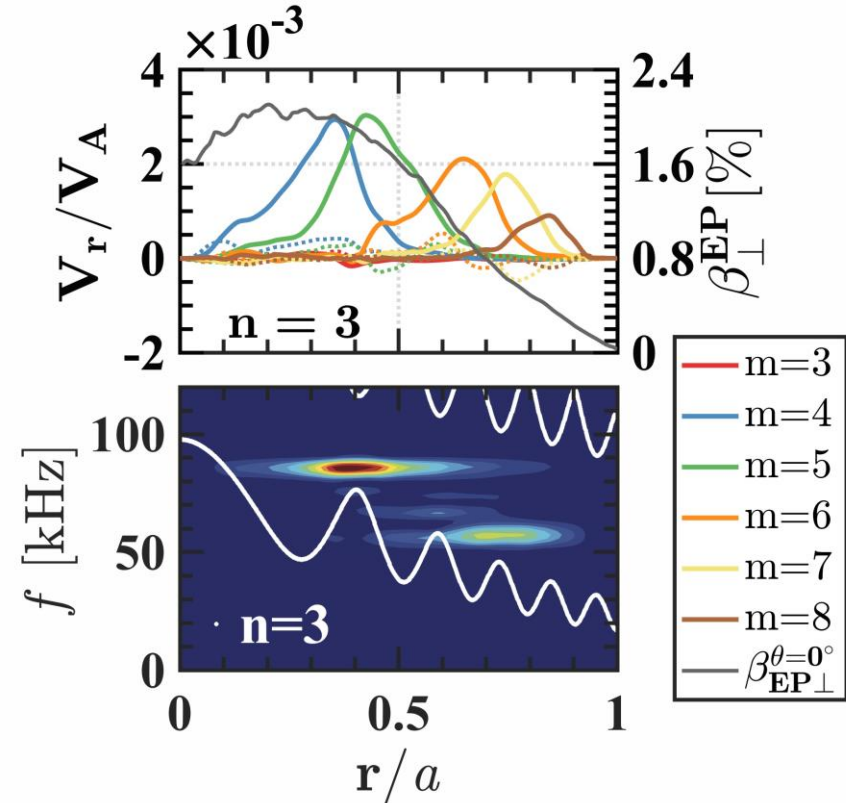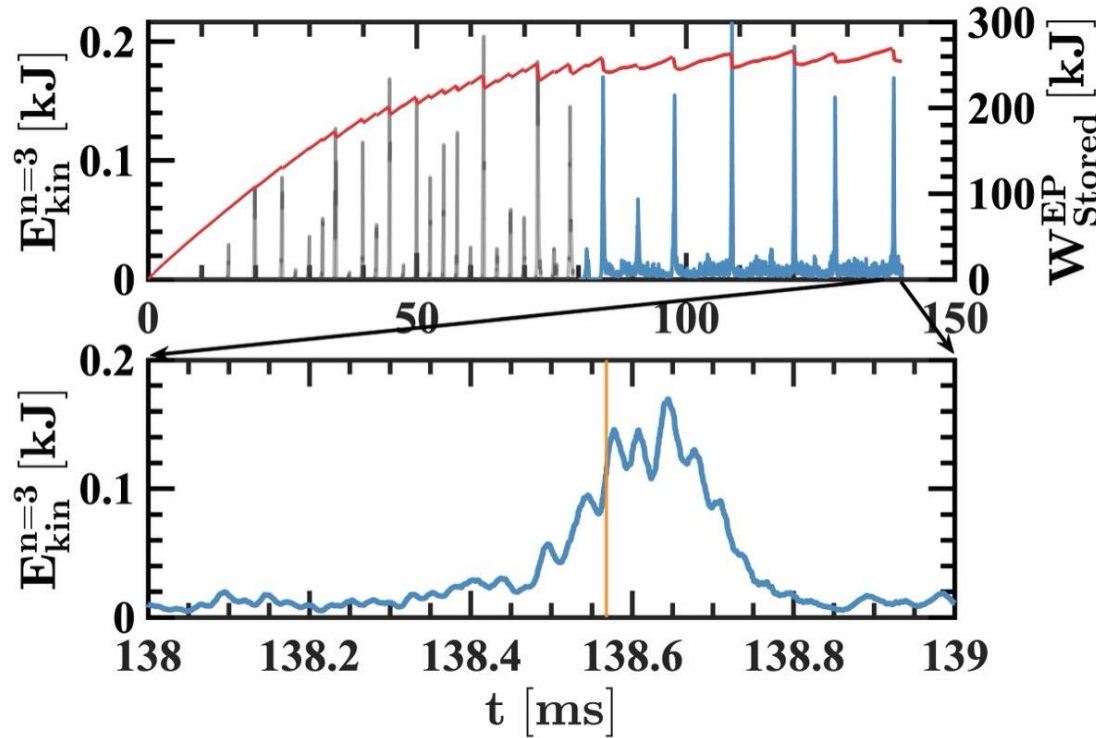**Single-*n* simulation with $n = 3$ toroidal mode family:** $n = 3$ mode is directly driven by fast particles, while $n = 0, 6, 9$ MHD perturbations are retained, which contribute to the TAE nonlinear saturation.

- **TAEs with a single *n* can also trigger the burst with a longer time interval of two adjacent bursts.**

- **Similar to the multi-*n* case, a series of discrete TAEs with different frequencies is formed.**

- **Oscillatory growth of kinetic energy results from different frequencies of inner and outer TAEs.**

Kinetic Energy Evolutions
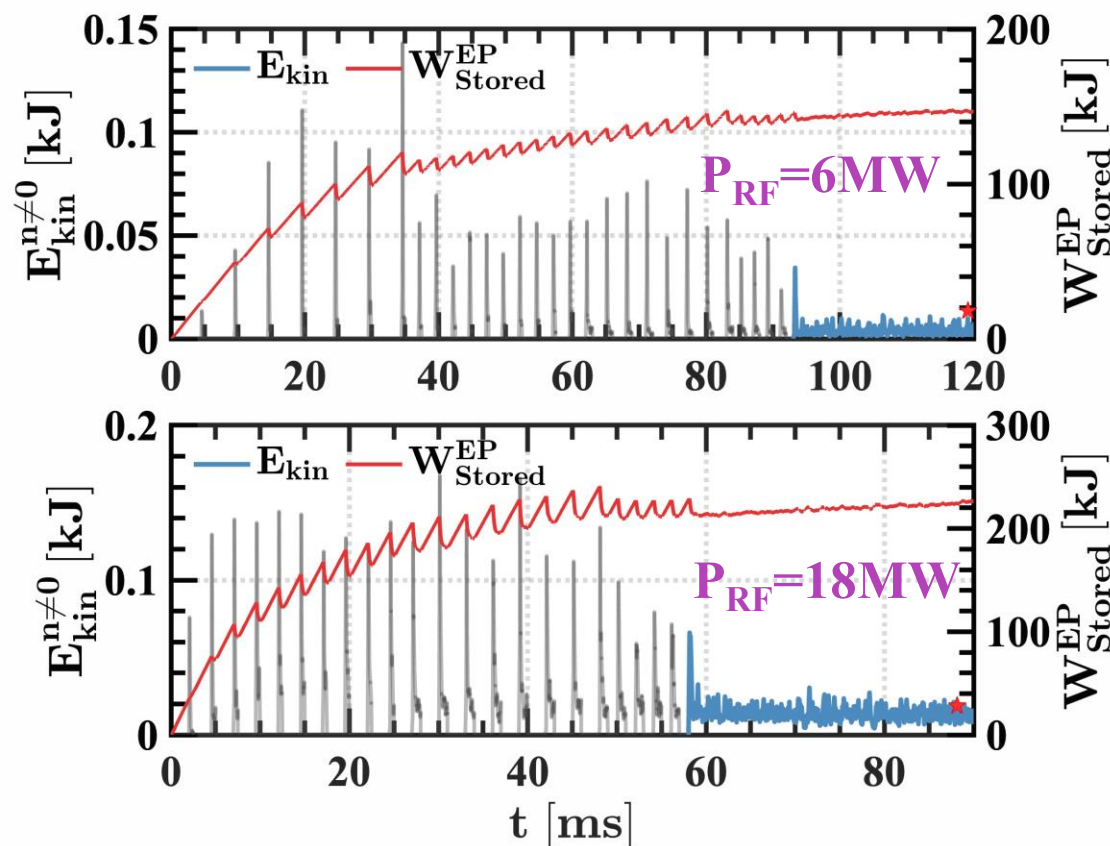
Minority Hydrogen Beta
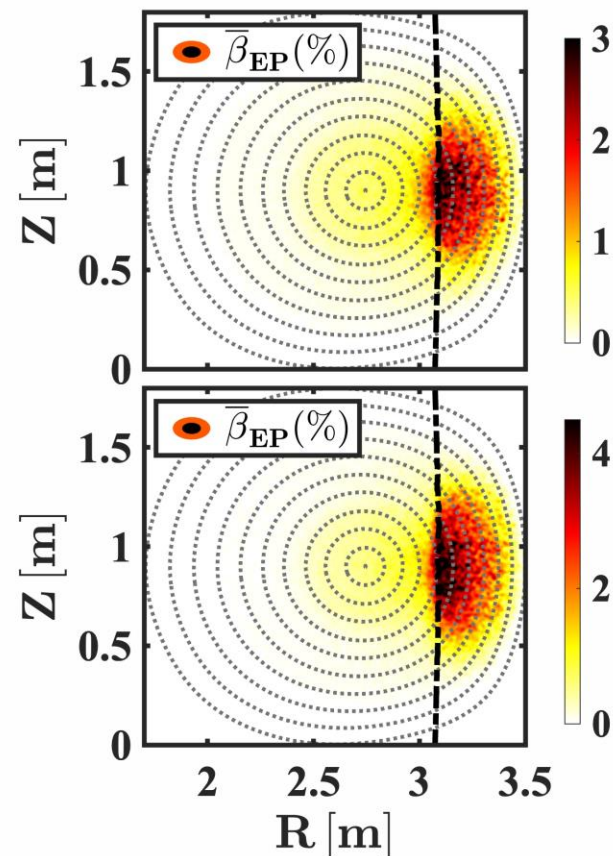
- When the RF resonance layer is located at the outboard region, only non-bursting/grassy modes are observed, even at a high power of 18MW.

- A significant number of minority ions are close to the RF resonance layer, indicating that resonant particles interacting with SAWs also easily experience strong RF-induced velocity space diffusion.

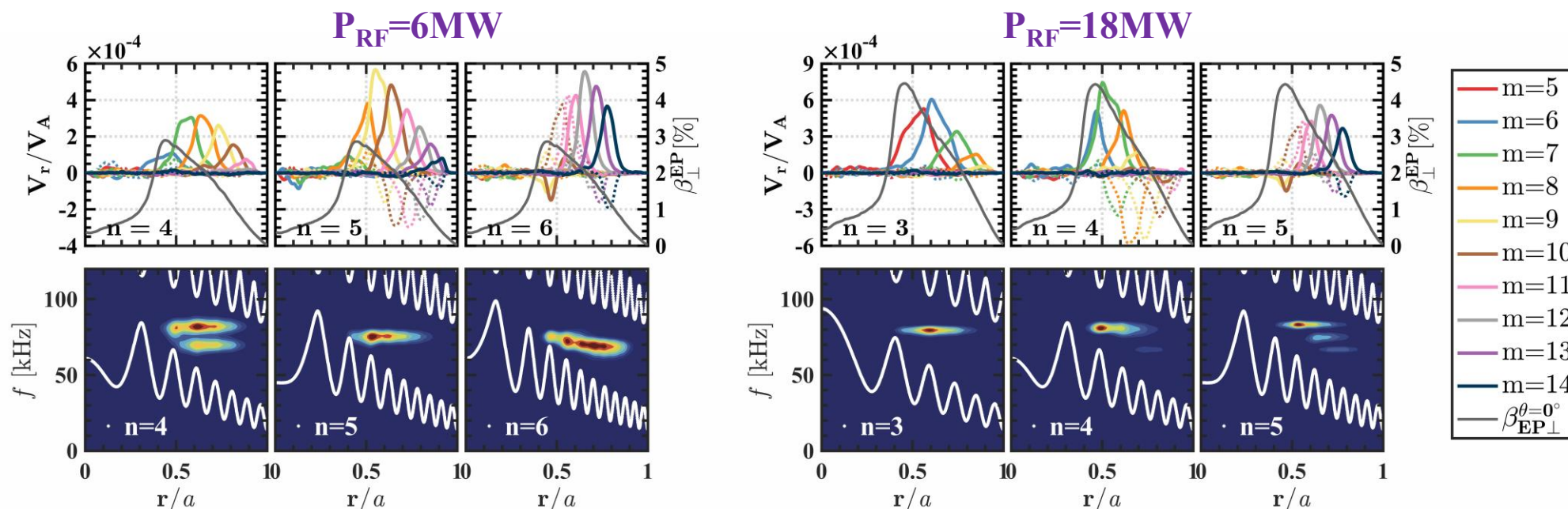- **For outboard RF heating, primary TAEs of each toroidal mode show a broad structure with almost identical frequency.**

- **RF-induced strong velocity space diffusion keeps scrambling resonant particles and preventing continuous particle trapping in the radial direction, which contributes to the formation of this broad structure with uniform mode frequency.**

- **Such a long-lasting broad structure will prevent the accumulation of free energy to trigger a bursting event.**

◆ **State-of-the-art hybrid particle-in-cell simulations of ICRF-induced AEs in tokamak plasmas are conducted, where both bursting and non-bursting AEs are reported.**

◆ **Bursting ICRF-induced AEs are obtained in both multi-n and single-n simulations for a plasma with a low magnetic field B_0=1.5T and an ICRF resonance layer located at the magnetic axis or inboard side.**

◆ **Formation of a series of discrete [discrete in both frequency and radial position: accumulate enough free enough before avalanche] but coherent [transport same group of EPs determined by resonance conditions] AEs plays a pivotal role in triggering the bursting event with a low magnetic field strength [large EP radial transport from inner to outer region by AEs], which can release a large amount of free energy stored in the minority ion distributions during the cascading avalanche.**

◆ **The results suggest that destruction of the coherent structure by scrambling resonant particles through fast-ion phase space engineering via RF waves could be a desirable strategy in preventing the bursting SAWs.**
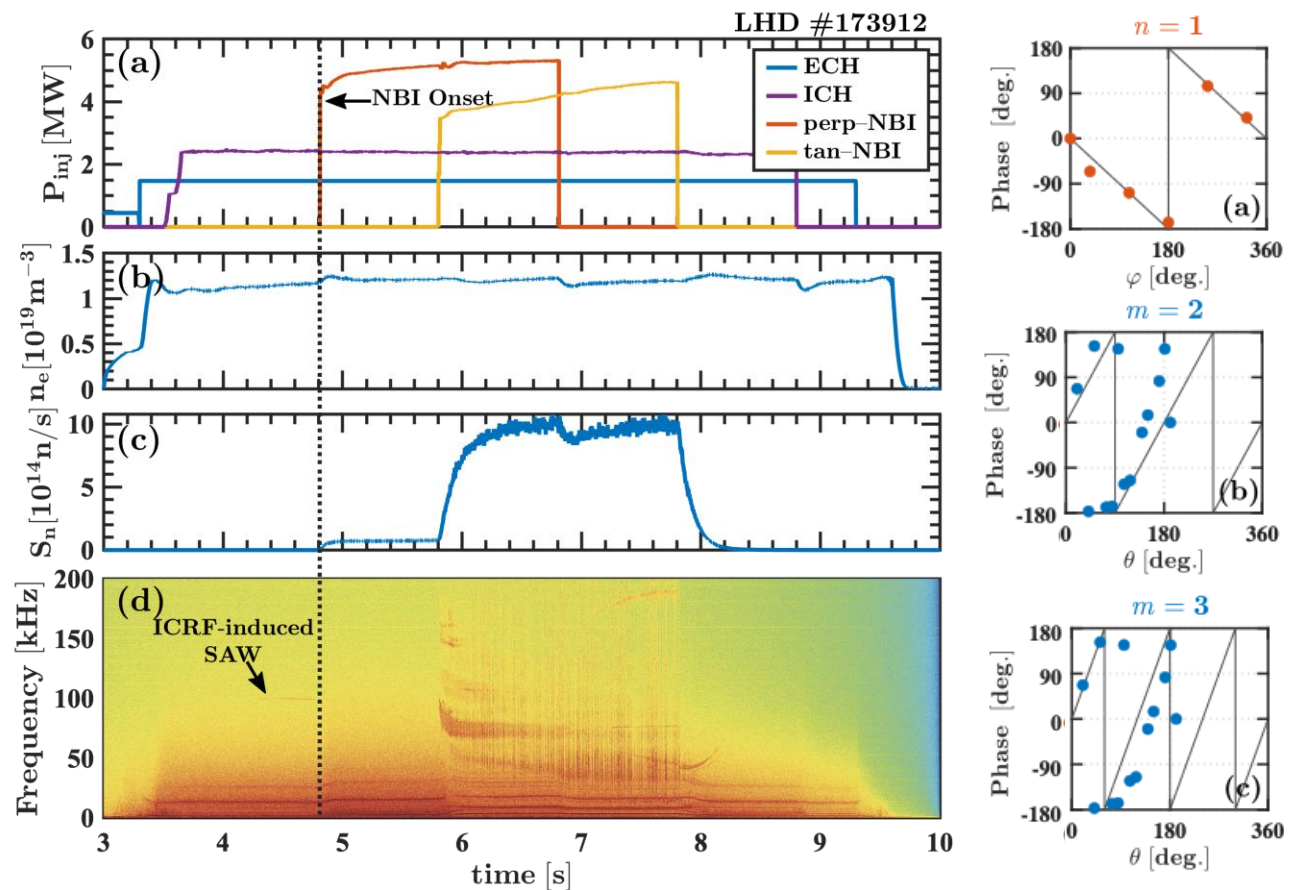
Thanks for your attention!

MEGA succeeded in predicting ICRF-induced SAW in LHD

MEGA predicted ICRF-induced SAWs in LHD
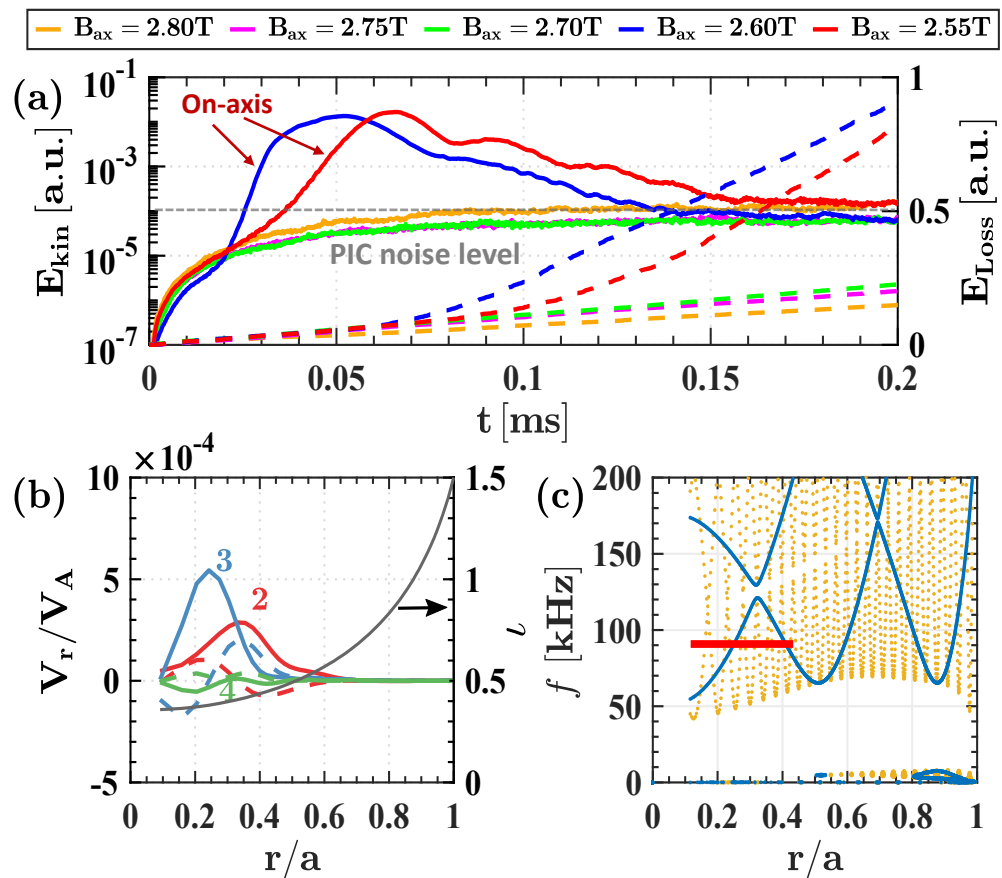
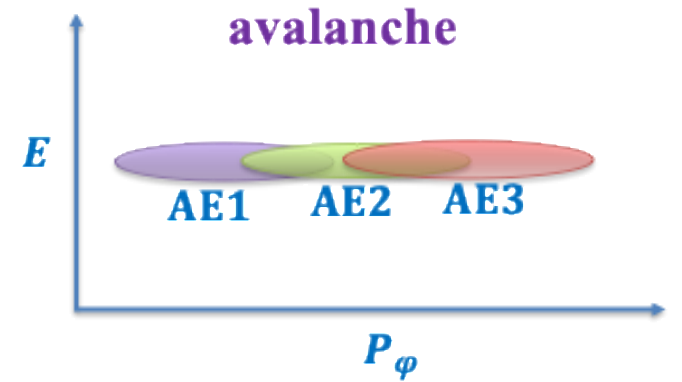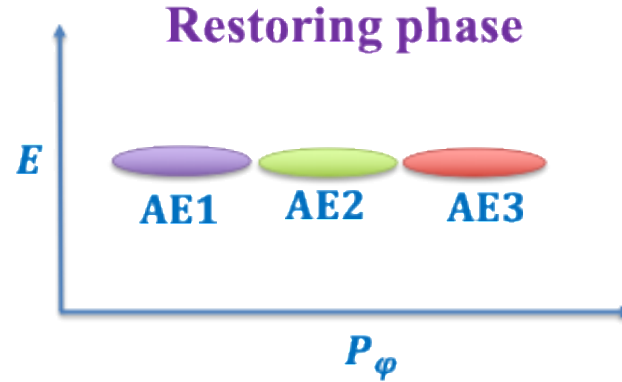**Experimental validation of ICRF-induced SAW in LHD**
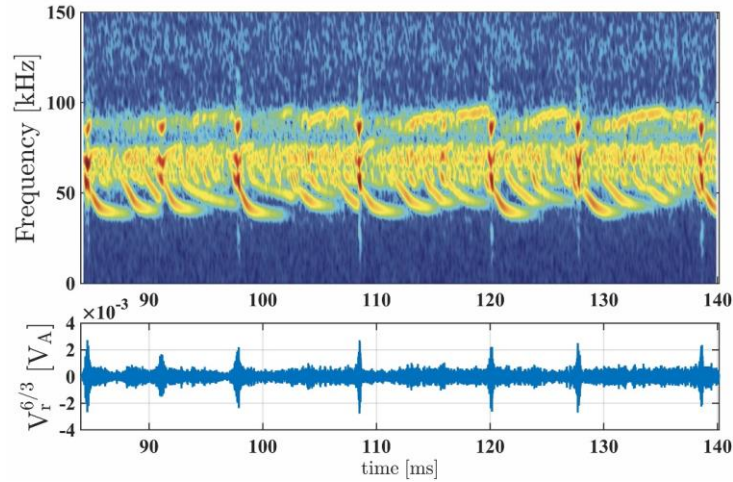

- **Extended MEGA has successfully predicted an ICRF-induced SAW in LHD.** [J. Wang+, FEC2023]

Single-*n* induced bursting SAWs

NBI-induced ALE
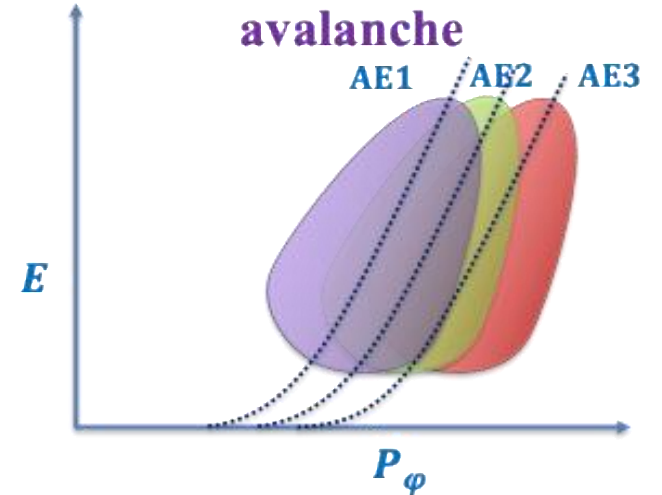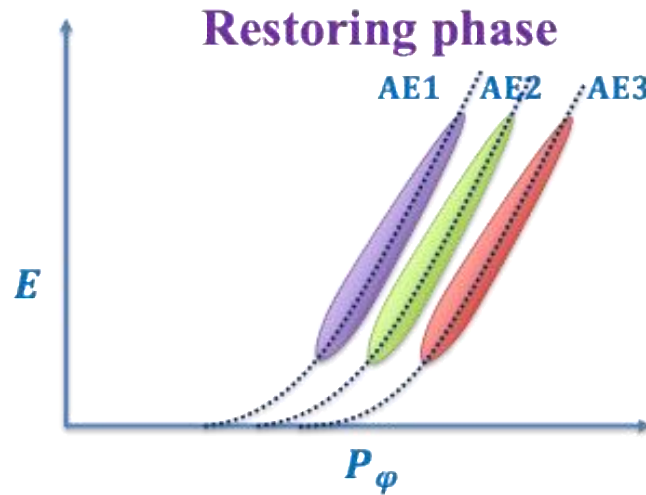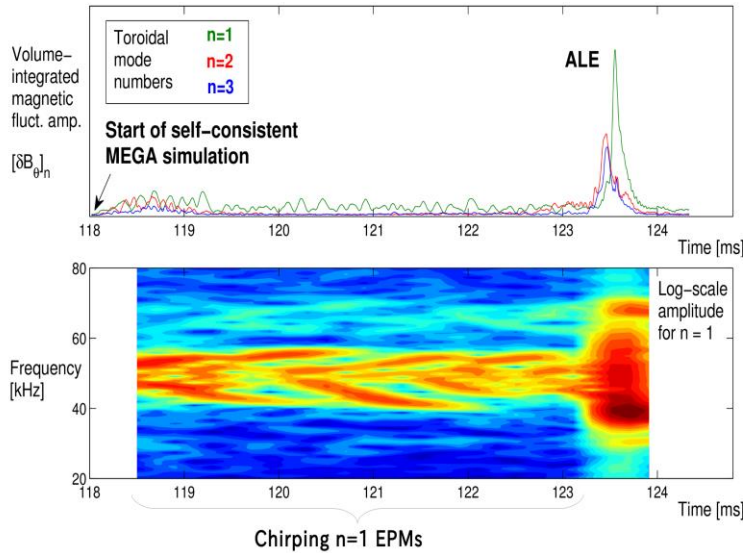
- **They share an identical fundamental triggering mechanism: resonance overlap in phase space**

Kinetic Energy Evolutions   **Minority Hydrogen Beta**   **Mode Structure**
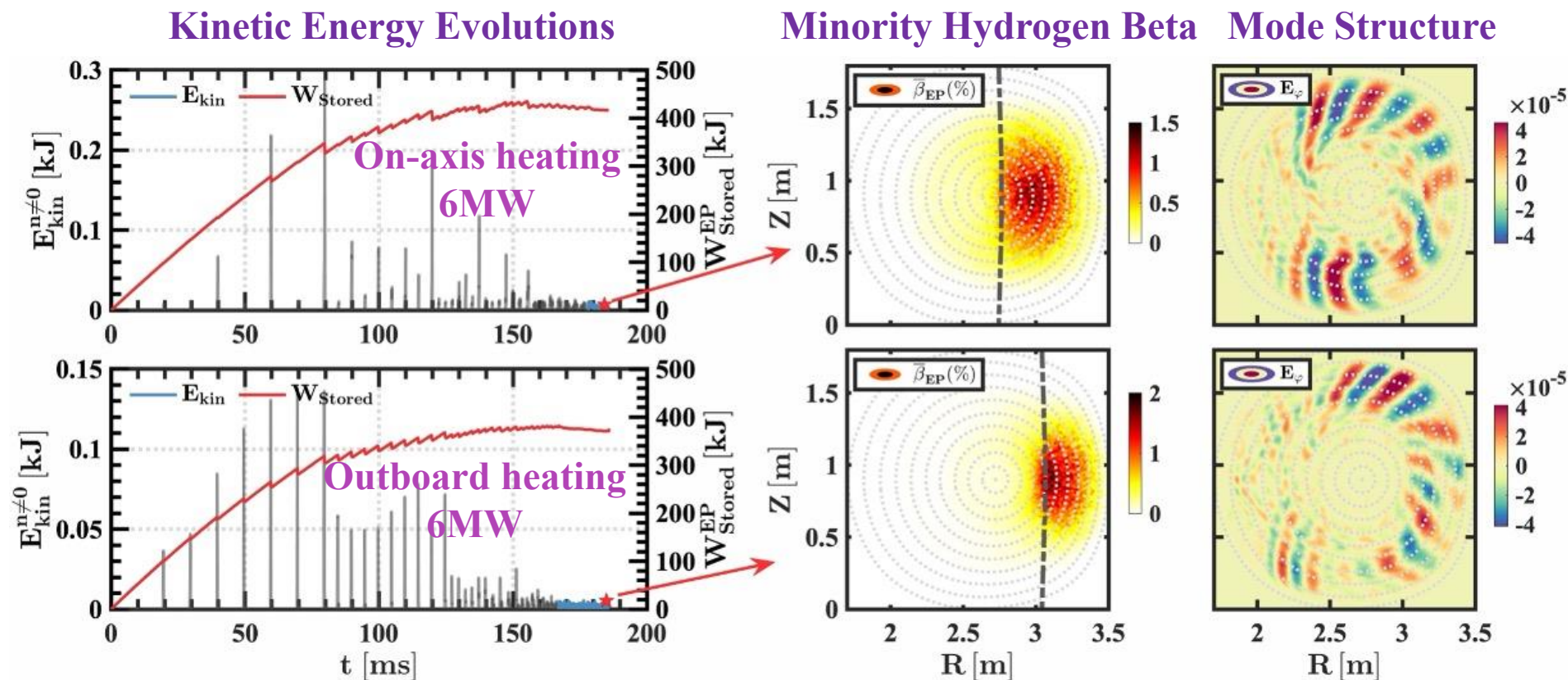
> **With a high magnetic field B$_0$=3.0T, only non-bursting/grassy modes are observed for both on-axis and outboard RF heating. [AEs remain non-bursting under on-axis heating, even with the enhanced P$_{RF}$ of 18 MW.]**

On-axis ICRF Heating [6MW]

rho/a=0.41
q_{loc}=1.50
(163kHz)

n=5, m= 8

rho/a=0.53
q_{loc}=1.70
(148kHz)

n=5, m= 9

rho/a=0.64
q_{loc}=1.93
(134kHz)

n=5, m= 10
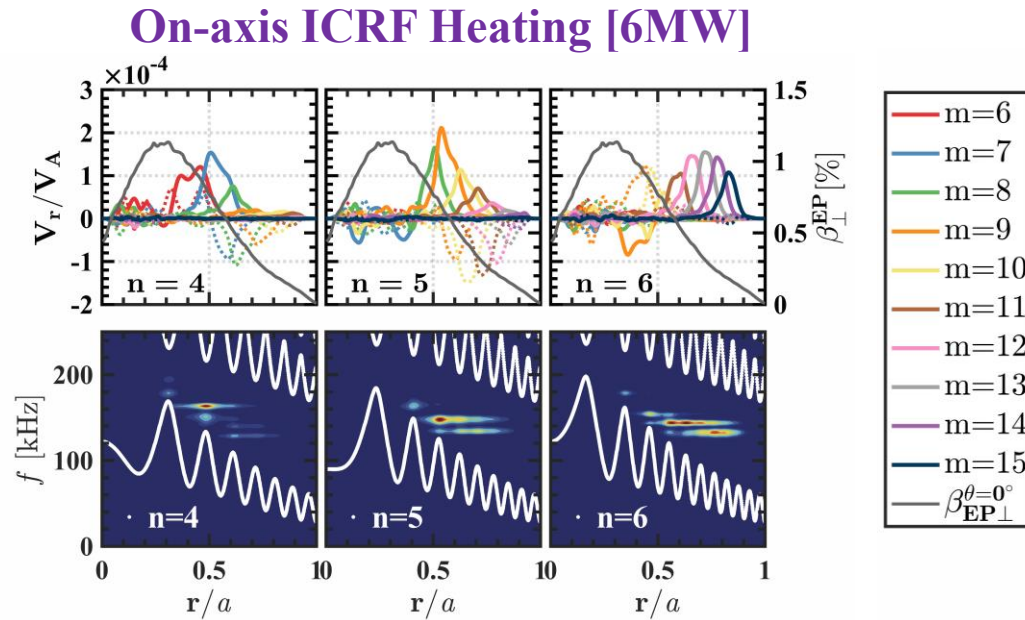
➤ Discrete AEs with different radial positions can still be formed for each toroidal harmonic, but with very broad spatial structure.

➤ Significant reduction of EP transport by doubling the magnetic field strength?
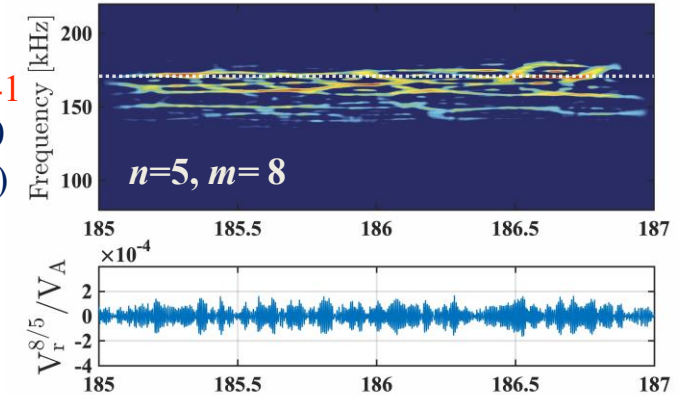
■ **RF kick: Kick in velocity space when minority particle crosses the Doppler-shifted resonance layer** (Stix, NF, 1975; Murakami+, NF, 2006) **:**

$$\Delta v_\perp = \frac{q}{2m_h} I \, exp(-in\phi_r)\,[|E_+|J_{n-1}(k_\perp \rho_h) + |E_-|J_{n+1}(k_\perp \rho_h)]$$

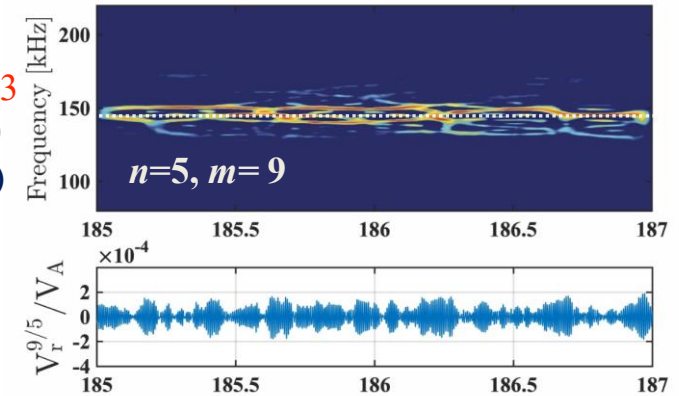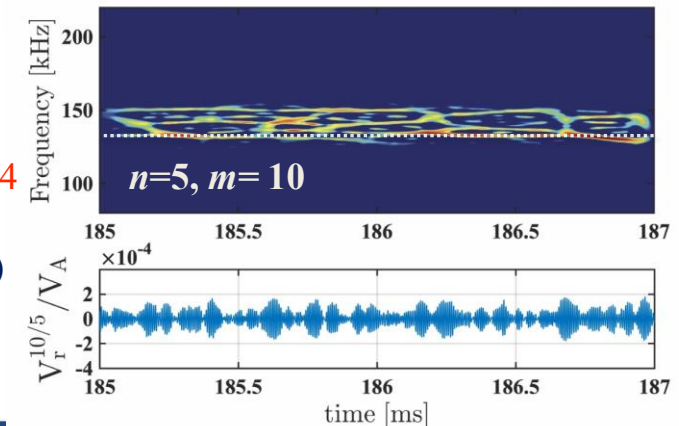- **RF kick is simulated by the Monte Carlo method.**

- **Wave-particle interaction time** $I = \min(t_1, t_2) = \min\left(\sqrt{2\,\pi/n\,\dot\omega}, 2\pi(n\,\ddot\omega/2)^{-1/3} \, Ai(0)\right)$ **depends on the turning point position relative to the resonance layer.** ($I = t_1$: **bounce tip far away from the resonance layer;** $I = t_2$: **bounce tip close to the resonance layer**)

- Random variable ϕ_r is the phase shift between the Larmor rotation and wave electric field.

- Left-hand polarized component of the perpendicular wave electric field E_+, which rotates in the direction of ion cyclotron motion, can effectively interact with the minority ions. A modeled E_+ profile is used in this work for simplicity.

- In this work, we focus on the fundamental minority ion heating scheme (n=1).

- **Source: A source module is implemented to maintain minority ion concentration**

- **Sink: Only particle orbit loss is considered in the present model**

- **Collisions: Minority ion (h) velocity change from $(v_\parallel, v_\perp)$ to $(v'_\parallel, v'_\perp)$ due to collisions with bulk ions and electrons (S)**(Karney, CPR,1986; Hamamatsu+, PPCF,2007)

$$v'_\parallel = v_\parallel + \Delta v_v^{h/S} \frac{v_\parallel}{v} - \Delta v_\chi^{h/S} \frac{v_\perp}{v}$$

$$v'_\perp = \left[\left(v_\perp + \Delta v_v^{h/S} \frac{v_\perp}{v} + \Delta v_\chi^{h/S} \frac{v_\parallel}{v} \right)^2 + \left(\Delta v_\eta^{h/S} \right)^2 \right]^{1/2}$$

Mean value and mean square derivation required in **Monte Carlo simulations**:
(velocity space is based on a spherical coordinate (v, χ, η) with Larmor phase η)

$$\left\langle \left(\Delta v_v^{h/S} \right)^2 \right\rangle = \frac{\Gamma^{h/S}}{2v} \left[\frac{\text{erf}(u)}{u^2} - \frac{\text{erf}'(u)}{u} \right] 2\delta t$$

$$\left\langle \Delta v_v^{h/S} \right\rangle = - \left(1 + \frac{m_h}{m_S} \right) \frac{\Gamma^{h/S}}{v^2} [\text{erf}(u) - u\text{erf}'(u)]\delta t$$

$$\left\langle \left(\Delta v_\chi^{h/S} \right)^2 \right\rangle = \left\langle \left(\Delta v_\eta^{h/S} \right)^2 \right\rangle = \frac{\Gamma^{h/S}}{4v} \left[\left(2 - \frac{1}{u^2} \right) \frac{\text{erf}(u)}{u^2} + \frac{\text{erf}'(u)}{u} \right] 2\delta t$$

$$\left\langle \Delta v_\chi^{h/S} \right\rangle = \left\langle \Delta v_\eta^{h/S} \right\rangle = 0$$